

Near Singular Integration

ISC 5238

April 24th, 2025



Contents

1 Introduction

2 Description of Methods

3 Numerical Testing

4 Conclusion/ Future work

Contents

1 Introduction

2 Description of Methods

3 Numerical Testing

4 Conclusion/ Future work

Introduction to Near-Singular Integration

• What is it?

- Evaluation of layer-potential integrals at points *close* to the integration surface
- Kernel behaves almost singularly \implies standard quadrature loses accuracy

Introduction to Near-Singular Integration

- **What is it?**

- Evaluation of layer-potential integrals at points *close* to the integration surface
- Kernel behaves almost singularly \implies standard quadrature loses accuracy

- **Why it matters?**

- Key step in boundary-integral solvers for Laplace, Helmholtz, Stokes, etc.
- Common in exterior field computations (e.g. electrostatics, viscous flow near walls)

Introduction to Near-Singular Integration

- **What is it?**

- Evaluation of layer-potential integrals at points *close* to the integration surface
- Kernel behaves almost singularly \implies standard quadrature loses accuracy

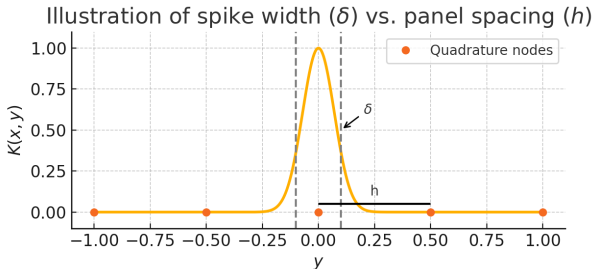
- **Why it matters?**

- Key step in boundary-integral solvers for Laplace, Helmholtz, Stokes, etc.
- Common in exterior field computations (e.g. electrostatics, viscous flow near walls)

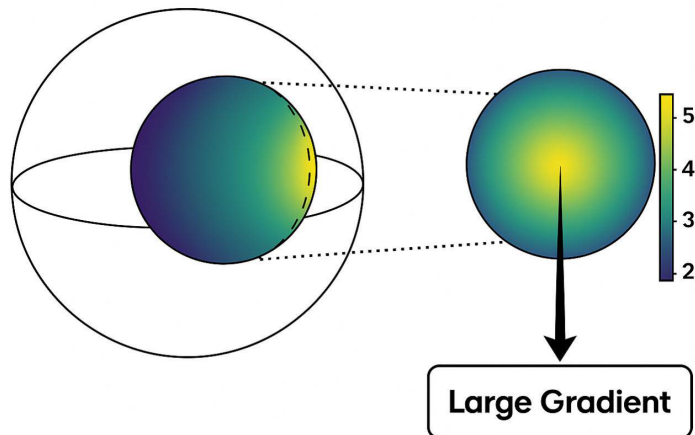
- **Why near-singular integrals are hard?**

Why Near-Singular Integrals Are Hard?

- Let x be a point a small distance δ from the surface Γ .
- The layer-potential kernel $D(x, y)$ remains *smooth* for $|x - y| \gg \delta$, but as $|x - y| \rightarrow \delta$ it
 - grows without bound
 - varies extremely rapidly over a length scale $\mathcal{O}(\delta)$
- If the panel size $h \gg \delta$, standard quadrature will produce large errors (it simply cannot “see” the sharp spike).



3D View



Contents

1 Introduction

2 Description of Methods

3 Numerical Testing

4 Conclusion/ Future work

- We consider several papers and extract their Near Singular methods.
- Previously, we have seen some of the methods shown
- We expand on the intuition gained to present additional methods



**Regularized Method
Expansion of Cauchy Integral**



Three Region Method



**QBX and
Differential Geometry
Approach**

Numerical Evaluation of Analytic Functions by Cauchy's Theorem loakimidis, Papadakis, and Perdios 1991

- Direct method using elementary quadrature rule with n nodes

$$\int_{\mathbb{C}} g(t) dt = \sum_{j=1}^n A_{jn} g(t_{jn}) + E_n(g) \quad (1)$$

- Where A_{jn} is the basis, $g(t_{jn})$ is our interpolated values and $E_n(g)$ is the correction term
- Think of this elementary method as the Trapezoidal method

- Indirect Approach, use of Taylor Series for points far away from the singularity

$$f(z) = \sum_{j=0}^{\infty} a_j (z - z_0)^j \quad (2)$$

- a_j is computed by

$$a_j = \frac{1}{j!} f^{(j)}(z_0) = \frac{1}{2\pi i} \int_C \frac{f(t)}{(t - z_0)^{j+1}} dt, \quad j = 0, 1, \dots \quad (3)$$

- Where the point z is substituted by the point z_0

$$f^{(m)}(z) = \sum_{j=0}^{\infty} a_j j(j-1)\dots(j-m+1)z^{j-m}, \quad m = 0, 1, \dots \quad (4)$$

- Method C
- Utilization of Cauchy's Theorem

$$\int_{\mathbb{C}} g(t) dt = 0 \quad (5)$$

- where $g(z)$ is analytic and without poles
- Applied to:

$$f(z) = \frac{1}{2\pi i} \int_{\mathbb{C}} \frac{f(t)}{t - z} \quad (6)$$

$$f^{(m)}(z) = \frac{m!}{2\pi i} \int_{\mathbb{C}} \frac{f(t)}{(t - z)^{m+1}} dt, \quad m = 1, 2, \dots \quad (7)$$

Sample Result

n	Method A: $f(z) - f_n(z)$	Method C: $f(z) - f_n(z)$
4	$(-3.0042 - i3.5419)E + 0$	$(-4.1124 - i0.7238)E - 2$
8	$(-1.2459 - i1.5693)E + 0$	$(-2.2418 - i0.2219)E - 4$
16	$(-4.9821 - i6.2782)E - 1$	$(-1.8076 - i0.0954)E - 11$
32	$(-1.5340 - i1.9331)E - 1$	absolutely $< 1.0E - 15$
64	$(-2.5347 - i3.1941)E - 2$	"
128	$(-0.9556 - i1.2042)E - 3$	"
256	$(-1.4646 - i1.8456)E - 6$	"

Figure: Numerical results for errors in $f(z)$ and $f'(z)$ with $f(z) = e^z$ by using the trapezoidal rule with $n = 2^q$ for an elliptic contour with semi-axes at $a = 2, b = 1$ and centered at 0, also $z = 0.9i$.

Extrapolated regularization of nearly singular integrals on surfaces Beal et al.

- The authors replace the singular kernel with a regularized version having a length parameter δ in order to control the discretization error
- For convergence as $h \rightarrow 0$ the authors choose δ proportional to h^q with $q < 1$
- This ensures that the discretization error is dominated by the regularization error

- This method can be applied to the double layer potential

$$\mathcal{D}(\mathbf{y}) = \int_{\Gamma} \frac{\partial G(\mathbf{x} - \mathbf{y})}{\partial \mathbf{n}(\mathbf{x})} g(\mathbf{x}) dS(\mathbf{x}) \quad (8)$$

- Using Green's identities, above can be rewritten as:

$$\mathcal{D}(\mathbf{y}) = \int_{\Gamma} \frac{\partial G(\mathbf{x} - \mathbf{y})}{\partial \mathbf{n}(\mathbf{x})} [g(\mathbf{x}) - g(\mathbf{x}_0)] dS(\mathbf{x}) + \chi(\mathbf{y})g(\mathbf{x}_0) \quad (9)$$

- Where \mathbf{x}_0 is the point closest to the boundary Γ , the authors set $\chi = 0$ for interior, $\chi = 1$ for the exterior and $\chi = 1/2$ for on the boundary Γ

- To regularize the authors replace ∇D with the gradient of the smooth function G_δ obtaining

$$\nabla G_\delta(\mathbf{r}) = \nabla G(\mathbf{r}) s_2\left(\frac{|\mathbf{r}|}{\delta}\right) = \frac{\mathbf{r}}{4\pi|\mathbf{r}|^3} s_2\left(\frac{|\mathbf{r}|}{\delta}\right) \quad (10)$$

- Where

$$s_2(r) = \operatorname{erf}(r) - \left(\frac{2}{\sqrt{\pi}}\right) r e^{-r^2}, \quad (11)$$

$$\operatorname{erf}(x) = \frac{2}{\sqrt{\pi}} \int_0^x e^{-t^2} dt \quad (12)$$

- Leaving us with:

$$\mathcal{D}_\delta(\mathbf{y}) = \int_{\Gamma} \frac{\mathbf{r} \cdot \mathbf{n}(\mathbf{x})}{4\pi|\mathbf{r}|^3} s_2\left(\frac{|\mathbf{r}|}{\delta}\right) [g(\mathbf{x}) - g(\mathbf{x}_0)] dS(\mathbf{x}) + \chi(\mathbf{y}) g(\mathbf{x}_0), \quad \mathbf{r} = \mathbf{x} - \mathbf{y} \quad (13)$$

Three-Region Method : Biros, Ying, and Zorin 2006

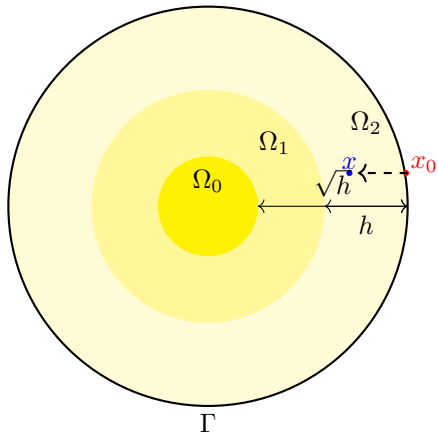


Figure: Domain partitioning.

$$(D\phi)(x) = \int_{\Gamma} D(x, y)\phi(y)dy, \quad \psi = \phi.J$$

Partitioning Evaluation Strategy

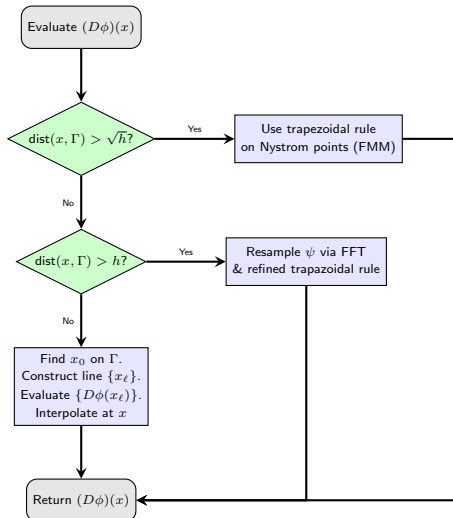
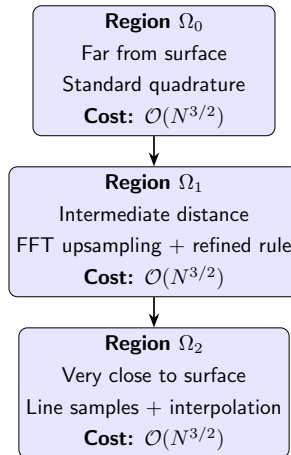


Figure: Corresponding evaluation strategies.

Three-Region Strategy and Cost



All regions maintain total cost $\mathcal{O}(N^{3/2})$, with high accuracy near boundary.

Limitations

- **Requires smooth surfaces:** Assumes that the boundary surface Γ is infinitely smooth (no sharp edges or corners).
- **Interpolation cost increases:** In Ω_2 , evaluating the integral at off surface points and performing high order Lagrange interpolation becomes computationally expensive for large L or fine grids.
- **Does not handle true singularities:** Designed for *nearly* singular integrals (when $x \notin \Gamma$ but is close). For singular integrals (when $x \in \Gamma$), separate singular quadrature schemes are still required.
- **Not adaptive:** The quadrature is based on uniform grids and fixed spacing h . Less effective for adaptive refinement or nonuniform discretizations.

Quadrature by expansion: Klöckner et al. 2013

- In this paper, the authors present a systematic, high-order approach that is designed to evaluate layer potentials, such as single- and double-layer potentials, which involve integrals with singular or weakly singular kernels. These potentials are defined as:

$$S\sigma(x) := \int_{\Gamma} G(x, x') \sigma(x') dx',$$
$$D\mu(x) := \int_{\Gamma} \frac{\partial G}{\partial \hat{n}_{x'}}(x, x') \mu(x') dx'$$

For target points x on a closed, smooth contour $\Gamma \subset \mathbb{R}^2$, where G is the Green's function for an underlying elliptic PDE and $\hat{n}_{x'}$ denotes the outward unit normal at x' . In the case of the double layer potential, it is typically the principal value of $D\mu$ that is desired for $x \in \Gamma$.

Quadrature by expansion: Klöckner et al. 2013

- QBX relies on the principle that the layer potentials are smooth away from the boundary. Although the integral kernels may be singular, the resulting potential field is smooth in the interior Ω^- and exterior Ω^+ domains.
- The author restricted their attention to the Helmholtz equation

$$\Delta\phi + k^2\phi = 0$$

for which

$$G(x, x') = \frac{i}{4} H_0^{(1)}(k|x - x'|),$$

where $H_0^{(1)}$ denotes the Hankel function of the first kind of order 0. $H_0^{(1)}$ satisfies the Sommerfeld radiation condition

$$\lim_{r \rightarrow \infty} r^{1/2} \left(\frac{\partial}{\partial r} - ik \right) H_0^{(1)} = 0$$

Quadrature by expansion: Klöckner et al. 2013

- **Local Expansion:** For a target point x on the boundary Γ , a nearby off-surface point c is chosen. The potential is then approximated by a local expansion (e.g., a series in Bessel functions for the Helmholtz equation) around c . For the Helmholtz equation, the local expansion takes the form:

$$\phi(x) = \sum_{l=-\infty}^{\infty} \alpha_l J_l(k\rho) e^{-il\theta}$$

Where: ρ, θ are polar coordinates of the target x with respect to the expansion center c . J_l are Bessel functions of order l .

Quadrature by expansion: Klöckner et al. 2013

- **Coefficient Computation:** The coefficients α_l in the local expansion are computed by integrating the kernel multiplied by the density function. For each expansion center c and for $l = -p, -p+1, \dots, p$, compute the coefficients α_l using a high-order quadrature rule:

Single layer:

$$\alpha_l = \frac{i}{4} \int_{\Gamma} H_l^{(1)}(k|x' - c|) e^{il\theta'} \sigma(x') dx'$$

Double layer:

$$\alpha_l^D = \frac{i}{4} \int_{\Gamma} \frac{\partial}{\partial \hat{n}_{x'}} H_l^{(1)}(k|x' - c|) e^{il\theta'} \mu(x') dx'$$

Where: $H_l^{(1)}$ are Hankel functions of the first kind. $(|x' - c|, \theta')$ are polar coordinates of x' with respect to c .

Quadrature by expansion: Klöckner et al. 2013

- The layer potential at the boundary point is then approximated by evaluating the local expansion at that point.
- The accuracy of QBX depends on factors like the order of the expansion (p) and the spacing of the quadrature nodes (h).

Quadrature by expansion: Klöckner et al. 2013

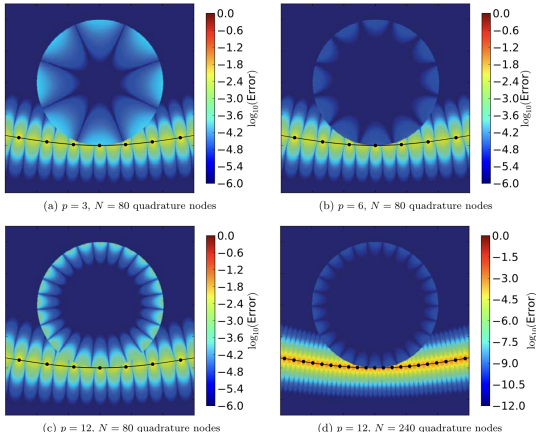


Fig. 3. The potential $S\sigma$ is computed using the trapezoidal rule I^* with either $N = 80$ or $N = 240$ points, except in a disk of radius $|c - x|$ centered at an off-surface point c that lies in the “high-accuracy” region of the trapezoidal rule (here, approximately $3h$ away from the curve in (a), (b), and (c)). Only a portion of the boundary I^* is plotted, and x is the point where the disk and I^* are tangent. We plot the error in the disk using various expansion orders p and numbers of quadrature nodes.

High Order close evaluation of Laplace Layer Potential:Zhu and Veerapaneni 2022

In this paper, the authors introduced a new method to solve the problem of close evaluation in three dimensions. They implemented the method for the double layer potential (DLP) that solves Dirichlet BVPs for the Laplace equation:

$$u(\mathbf{r}') = \mathcal{D}[\mu](\mathbf{r}'), \quad \mathcal{D}[\mu](\mathbf{r}') = \int_{\mathcal{M}} \frac{(\mathbf{r}' - \mathbf{r}) \cdot \mathbf{n}_{\mathbf{r}}}{4\pi|\mathbf{r}' - \mathbf{r}|^3} \mu(\mathbf{r}) dS_{\mathbf{r}}.$$

This can be expressed using exterior 2-forms for componentwise analysis:

$$\frac{(x' - x)\mu}{4\pi|\mathbf{r}' - \mathbf{r}|^3} dy \wedge dz + \frac{(y' - y)\mu}{4\pi|\mathbf{r}' - \mathbf{r}|^3} dz \wedge dx + \frac{(z' - z)\mu}{4\pi|\mathbf{r}' - \mathbf{r}|^3} dx \wedge dy$$

High Order close evaluation of Laplace Layer Potential:Zhu and Veerapaneni 2022

Using Poincaré's Lemma :

$$\omega = \left(\int_0^1 (tzg_2 - tyg_3) dt \right) dx + \left(\int_0^1 (txg_3 - tzg_1) dt \right) dy + \left(\int_0^1 (tyg_1 - txg_2) dt \right) dz$$

Using the definition of a quaternion $g = g_0 + g_1\mathbf{i} + g_2\mathbf{j} + g_3\mathbf{k}$., the kernel and density product is expressed as:

$$\alpha = \frac{(\mathbf{r}' - \mathbf{r}) \cdot \mathbf{n}(\mathbf{r})}{|\mathbf{r}' - \mathbf{r}|^3} f(\mathbf{r}) dS_{\mathbf{r}}.$$

This enables a systematic reduction to 1-form using Stokes.

High Order close evaluation of Laplace Layer Potential:Zhu and Veerapaneni 2022

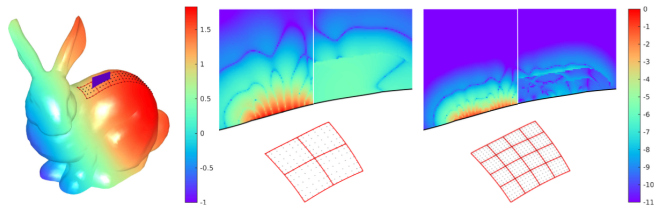


FIG. 1. One of the key advantages of the close evaluation scheme developed in this paper is its ease of handling arbitrary meshes. Here, we demonstrate its performance on the Stanford bunny triangulation data [27]. We used the interactive sketch-based quadrangulation method of [24] to create high-quality quad remeshings locally as shown on the top of the bunny. We evaluate the DLP at targets that are located arbitrarily close to the surface as shown on top in blue color. The surface is colored by the density function μ , which was set as $\mu(x, y, z) = e^{xy} - 1 + x + \sin(x^4 + 1/2y^3) + y - 1/2y^2 + 1/5y^6 + z$. Middle and right: Given this setup, we demonstrate the performance of the new scheme by considering one of the quads, successively refining it twofold and visualizing the errors due to direct evaluation of DLP via the high-order smooth quadrature rule (left half) and the new close evaluation scheme (right half). We note that, while the errors stagnate in a band close to the surface in the case of smooth quadrature, the new scheme achieves uniform accuracy up to 10 digits. This is a self-convergence test compared with a reference solution obtained on an 8×8 panel refinement of the quad. More details on this experiment are provided in section 5.

High Order close evaluation of Laplace Layer Potential:Zhu and Veerapaneni 2022

- On analytic test functions, the scheme achieves **7th-order convergence**.
- Close evaluation accuracy does not degrade near the boundary — errors remain small and uniform.
- On complex geometries, the method handles unstructured meshes robustly.
- Achieves up to **10-digit accuracy** for targets arbitrarily close to the surface.

Contents

1 Introduction

2 Description of Methods

3 Numerical Testing

4 Conclusion/ Future work

Numerical Testing

- Here we aim to solve the Cauchy's Integral Formula

$$f(a) = \frac{1}{2\pi i} \int_{\gamma} \frac{f(z)}{z-a} dz \quad (14)$$

where γ is the boundary of any disc $D \subset \mathbb{C}$ and $a \in D$.

- In this problem we have a pole of order 1 when $z = a$
- For the test function we consider

$$f(z) = e^z \sin(z^2) + 1 \quad (15)$$

Integrand Plots

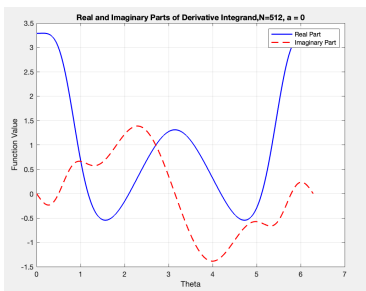
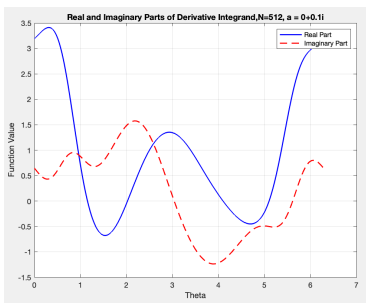
(a) $a = 0$ (b) $a = 0.1i$ 

Figure: Plots for the real and imaginary parts of the Integrand $\frac{f(z)}{z-a} dz$ with $f(z) = e^z \sin(z^2) + 1$. Here we vary a closer to the boundary of the unit disk

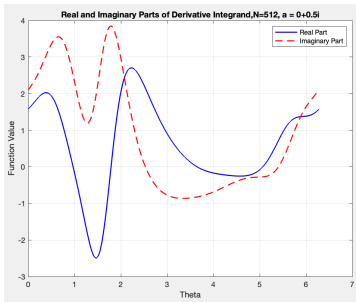
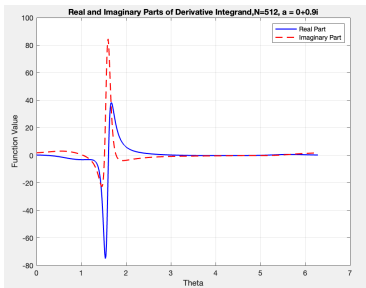
(a) $a = 0.5i$ (b) $a = 0.9i$ 

Figure: Plots for the real and imaginary parts of the Integrand $\frac{f(z)}{z-a} dz$ with $f(z) = e^z \sin(z^2) + 1$. Here we vary a closer to the boundary of the unit disk

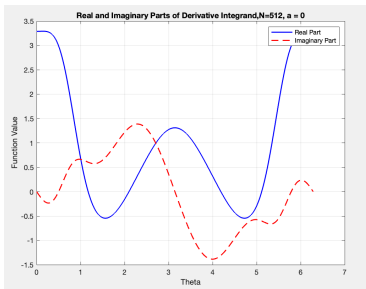
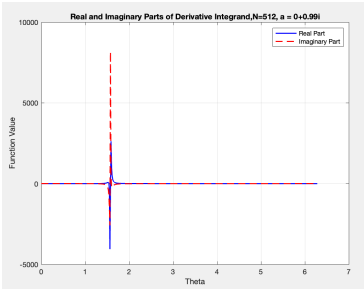
(a) $a = 0$ (b) $a = 0.99i$ 

Figure: Plots for the real and imaginary parts of the Integrand $\frac{f(z)}{z-a} dz$ with $f(z) = e^z \sin(z^2) + 1$. Here we vary a closer to the boundary of the unit disk

Project II Testing

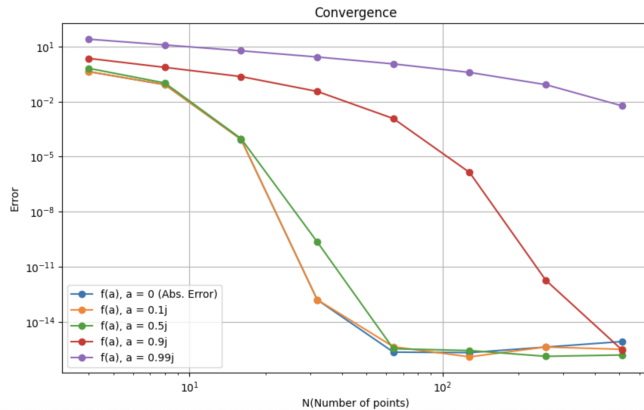


Figure: Convergence study varying the singular point on log-log scale.

Contents

1 Introduction

2 Description of Methods

3 Numerical Testing

4 Conclusion/ Future work

Future Work

- Here we have studied a survey of methods pertaining to solving these near singular integration issues. A few expansions which we wish to implement in the future are:
 - ① We will implement the three-region method, regularization method, and the differential geometric approach discussed.
 - ② We will compare all of the methods and perform a detailed convergence analysis.
 - ③ We aim to conduct a comprehensive review of the methods discussed in this study.
 - ④ Try additional functions to study convergence and analysis
 - ⑤ Possibly use them in our own research

References I

-  Beale, J. Thomas and Svetlana Tlupova (2024). "Extrapolated regularization of nearly singular integrals on surfaces". In: *Advances in Computational Mathematics* 50.4, p. 61. DOI: 10.1007/s10444-024-10161-4. URL: <https://doi.org/10.1007/s10444-024-10161-4>.
-  Biros, George, Lexing Ying, and Denis Zorin (2006). "A Fast Algorithm for the Evaluation of Nearly-Singular Layer Potentials". In: *Journal of Computational Physics* 212.1, pp. 132–156.
-  Ioakimidis, N. I., K. E. Papadakis, and E. A. Perdios (1991). "Numerical evaluation of analytic functions by Cauchy's theorem". In: *BIT Numerical Mathematics* 31.2, pp. 276–285. DOI: 10.1007/BF01931287. URL: <https://doi.org/10.1007/BF01931287>.

References II

-  Klöckner, Andreas et al. (2013). "Quadrature by expansion: A new method for the evaluation of layer potentials". In: *Journal of Computational Physics* 252, pp. 332–349. ISSN: 0021-9991. DOI:
<https://doi.org/10.1016/j.jcp.2013.06.027>. URL: <https://www.sciencedirect.com/science/article/pii/S0021999113004579>.
-  Ying, Lexing, George Biros, and Denis Zorin (2006). "A high-order 3D boundary integral equation solver for elliptic PDEs in smooth domains". In: *Journal of Computational Physics* 219.1, pp. 247–275. ISSN: 0021-9991. DOI:
<https://doi.org/10.1016/j.jcp.2006.03.021>. URL: <https://www.sciencedirect.com/science/article/pii/S0021999106001641>.

References III

-  Zhu, Hai and Shravan Veerapaneni (2022). "High-Order Close Evaluation of Laplace Layer Potentials: A Differential Geometric Approach". In: *SIAM Journal on Scientific Computing* 44.3, A1381–A1404. DOI: 10.1137/21M1423051. eprint: <https://doi.org/10.1137/21M1423051>. URL: <https://doi.org/10.1137/21M1423051>.



Thank You Any Questions?